Using high power CSEM during the Energy Transition

K. Strack KMS Technologies, Houston

When asking yourself what will be the biggest contribution during the future energy transition for electromagnetics(EM) , one quickly reaches monitoring of reservoir fluid for CO2 and geothermal. Not so obvious is the application to enhance oil recovery where EM can reduce the carbon footprint by 30 to 50%. Methods and technologies such as electromagnetics (EM) have gained interest driven by their sensitivity to changes in reservoir fluids.

The prime depth range for these applications is 1 to 5 km and since fluid anomalies are small a higher accuracy is measurement and interpretation is require than hereto customary.

We developed over the last decades equipment (KMS array acquisition system) and a high power transmitter (100 and 150 KVA) to address that. Using application examples, a generalized workflow is implemented for waterflood injection, CO_2 storage monitoring, and geothermal exploration using the system. Key is the constant validation (comparing to logs) via examples from a waterflood injection monitoring using controlled-source electromagnetic (CSEM) in Asia and CSEM and magnetotellurics (MT) baseline surveys for CO_2 application in North Dakota, USA.

Reservoir Monitoring Workflow

Reservoir monitoring requires a proper strategy to verify the monitoring results. Figure 1 shows a CSEM reservoir monitoring workflow developed for waterflood and CO_2 injection monitoring studies. The workflow's input data include interpreted horizons from seismic, well logs covering the reservoirs of interest (up to a maximum depth of ~4000 m in highly resistive areas), and field noise measurements.

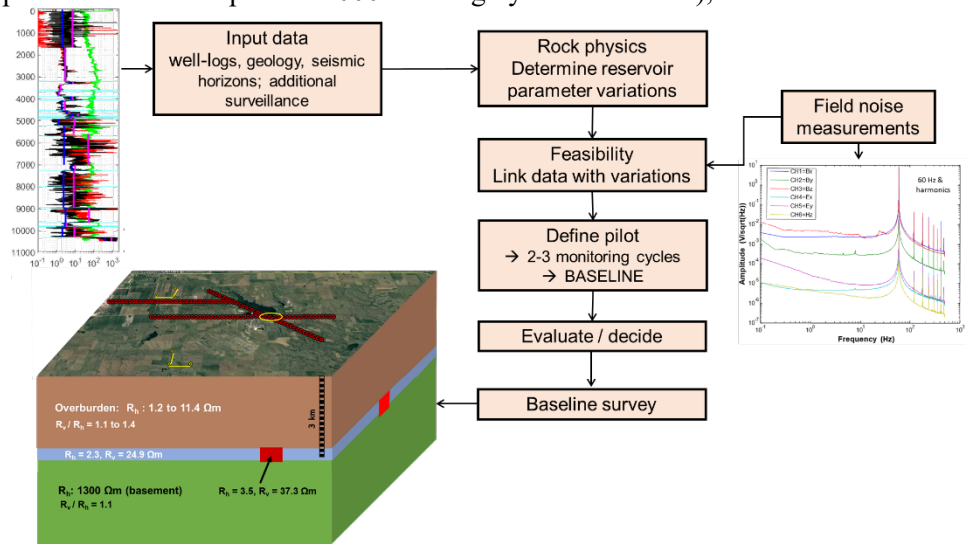

Figure 1 *CSEM generalized reservoir monitoring workflow for surface measurements (after Bararja-Olalde et al., 2021).*

In the first step of the workflow, a homogeneous layered resistivity model is generated, both for the horizontal and vertical resistivity. The horizontal and vertical resistivities can be upscaled from multi-directional resistivity well logs; otherwise, an anisotropic model based on the algorithms for cumulative total electrical conductance and total cumulative resistance can be generated (Keller and Frischknecht, 1967; Strack, 1992). An anisotropic model example is shown in Figure 2. Additional well logs are analyzed, and a fluid substitution (using Archie's equation) is carried out by replacing the saturating fluid with either water, brine, oil, or CO_2. The generated 1-D anisotropic model is then used to build the 3D model considered in the monitoring or exploration scenarios.

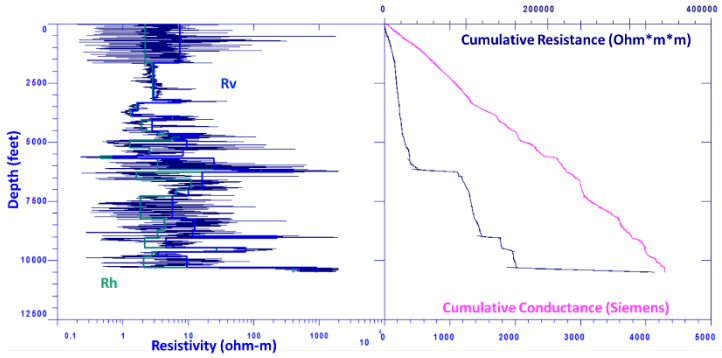

Figure 2 *Anisotropic model generated from the cumulative conductance and transverse resistance curves. Left: dark blue - composite resistivity log, blue and green curves are the equivalent model for vertical resistivity (Rv) and horizontal resistivity (Rh), respectively. Right: dark blue - cumulative resistance and magenta - cumulative conductance corresponding to Rv and Rh curves.*

Field Noise Measurements

Prior to the 3D modeling, field measurements are conducted to assess noise conditions. The noise information allows optimization of the survey design and estimation of the data's signal-to-noise ratio. All components (system and sensors) used in data acquisition are tested, including different magnetic field sensors, such as the LEMI-120 induction coil and the KMS S20 air loop. The goal is to utilize the most sensitive equipment for detecting small resistivity variations from the fluid change. An example of the amplitude spectrum of CSEM and MT noise measurements is shown in Figure 3. The amplitude of the noise recorded by the induction coils is higher than the air loop's noise. This difference suggests that the areal averaging of the air coil reduces some of the localized noise. The power line noise at 60 Hz and its harmonics observed in the raw data are attenuated during data processing. Subsequently, the air coil data are used to simulate noise combined with the transmission cycle and signal processing.

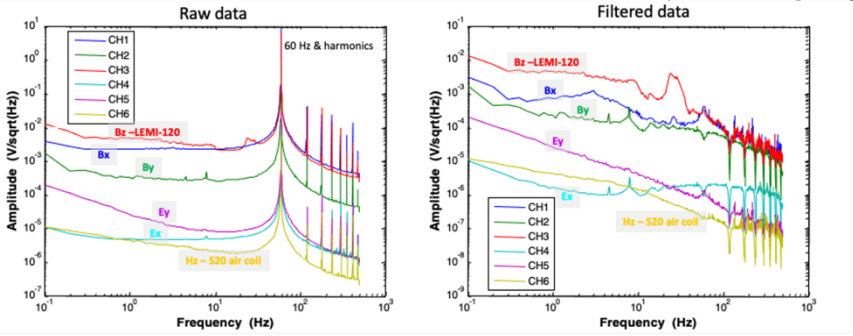

Figure 3 *Amplitude spectra of noise measurements for raw data (left) and after filtering power line noise (right). Colors represent different EM sensors. The red curve is for the LEMI-120 magnetic field coil, and the yellow curve corresponds to the KMS S20 air loop coil.*

3D Modeling

3D modeling is the core for understanding whether CSEM can detect changes in resistivity from the saturating fluid from the reservoir layers and define the optimum hardware to record such signals. Also, by integrating field noise measurements, one can determine whether the signal changes can be resolved in the presence of local noise, a critical element in highly cultural noise areas.

Commonly for CSEM 3D modeling, a transmitter location with characteristics such as the KMS' 5100 150 kW transmitter and an array of receivers, similar to the KMS'-820 system with two horizontal electric field components and one vertical magnetic field near the injection site, are simulated for various 3D models corresponding with the different scenarios either of a waterflood or CO_2 substitution. The 3D modeling code is benchmarked against the 1D solutions to assess numerical noise and the noise caused by the modeling grid's approximation errors. The benchmark models covering most of the field

scenarios are based on petrophysical analysis such as changes in resistivity due to the fluid substitution, percentage of the saturating fluid (a range is tested), and the capacity of the reservoir to store a certain volume. The equipment/sensor choice is added to minimize the 3D modeling effort. The result is a set of models including the expected anomaly within the measurable time window.

After modeling the different scenarios, one can determine the minimum percent change of saturating fluid and flood radius that produces a significant strong anomaly to be detected and the optimal receiver spacing to reconstruct the curve variation properly. Next, a reference representing the local noise measured in the field is added to the 3D modeling results. Figure 4 shows an example of one of the modeling scenarios of a CO_2 injection monitoring study. The strongest signal is from the electric component in the X direction; however, all field components show responses above the noise level.

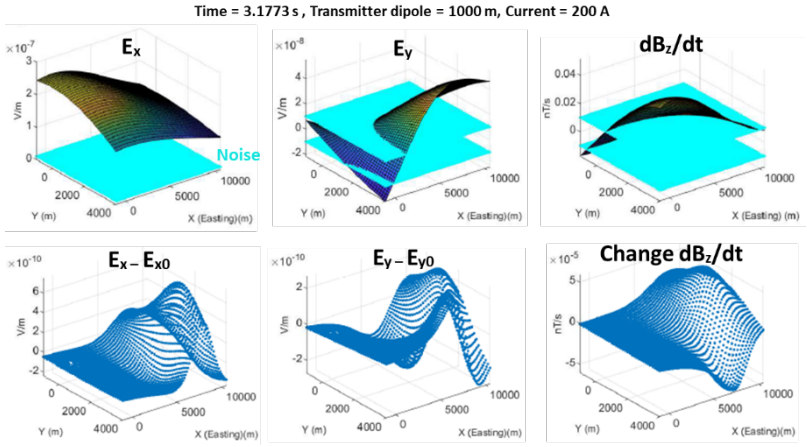

Figure 4 *3D modeling results for a scenario where a reservoir layer has been injected with CO_2. The receiver is located above the injection zone. Top images show the field response for the Ex (left), Ey (middle), and dBz/dt (right) components. Bottom images are the difference in response before and after the injection scenario modeled. The transmitter is in the x-direction. The field noise level was added (cyan surface); all components show responses above the noise level (after Bararja-Olalde et al., 2021).*

Workflow validation

We analyzed the results obtained from the 3D modeling against the acquired field data from a waterflood and CO_2 storage examples to validate the workflow. The recorded data are uploaded to the cloud in real-time during acquisition, and a field geophysicist does quality assessment and quality control to ensure data satisfy the pre-established quality standards. During data processing, noise in the survey area is analyzed to ensure that previous noise measurements used during the modeling are within the same range. Next, MT (when available) and CSEM data are inverted; the results from 1D inversions are expected to be similar to the original anisotropic model derived from the well logs. For baseline measurements, checking the recorded noise and signal is crucial to see whether they are similar to those simulated and equally important to fine-tune the 3D model used to plan the time-lapse measurement. Figure 7 shows the results of the vertical magnetic field component measurements from a receiver located on top of a steam injection site for EOR before and after steam is injected; the change in signal is significant (~30%). Figure 8 shows an example of the 1D inversion results of MT field data for the baseline survey of a CO_2 injection project. The results corroborate the quality of the model used for the simulation of the fluid substitution.

Ultimately, the complete validation of the workflow occurs after multiple time-lapse measurements. As some of the projects are still in their early stages, we do not have enough time-lapse data yet; however, the initial results from the waterflood study shows CSEM is capable of detecting the changes in fluid, and once the field information is feedback into the simulation models the question to ask now is: how small fluid changes can CSEM detect?

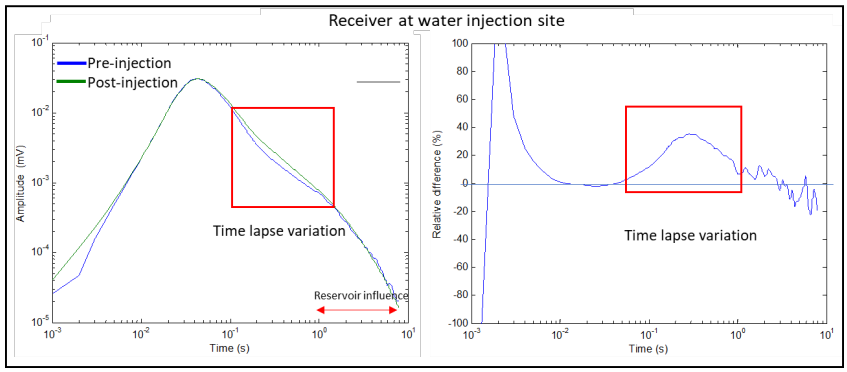

Figure 7 *Left: CSEM field data of the vertical magnetic field for waterflood before (blue) and after (green) steam injection. Right: percent change between the two measurements.*

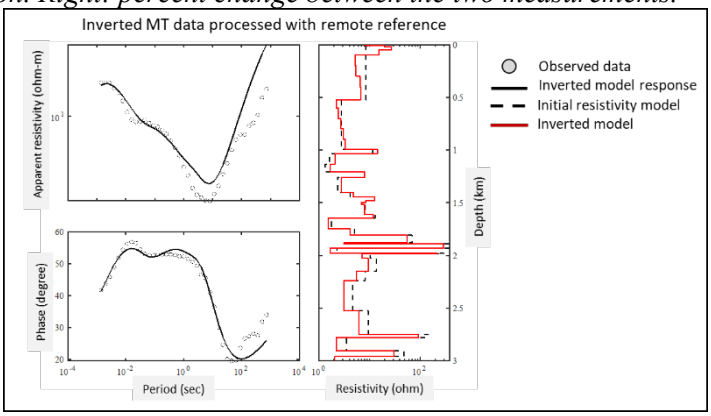

Figure 8 *1D inversion results of MT field data vs. the response of the initial anisotropic model used for the 3D modeling for CO_2 injection.*

Conclusions

Electromagnetic methods continuously prove to have better sensitivity to the bulk resistivity resulting from changes in the reservoir fluid than any other geophysical method. CSEM is among the best for EOR and CO_2 storage reservoir monitoring applications. CSEM shows good sensitivity to depths between 200 - 3500 m, representing the range of depth for the reservoirs of interest. Advances in hardware and data processing have also made it possible to accurately measure small fluid changes in real field conditions. A generalized workflow to carry 3D modeling and field noise measurements has shown through real data examples to be a good approach at understanding time-lapse surveys, coupled with selecting the optimal hardware for increasing signal-to-noise ratio during acquisition. Examples from a waterflood monitoring in Asia and preliminary results for a baseline survey for CO_2 injection in North Dakota, USA, show the model's appropriateness and the potential of CSEM to detect water or CO_2 flood fronts. Further validation of the workflow is expected after several more time-lapse measurements are completed.

Acknowledgments

The authors want to thank our colleagues from KMS Technologies and the University of North Dakota-EERC and the support of Minnkota Power Cooperative *and the US Department of Energy.* I appreciate and acknowledge the support of C. Baraja-Olalde, S. Davydycheva, T. Hanstein, Y. Martinez, A.Y. Paembonan, H. Passalacqua, M. Smirnov, and X. Xu in carried out this work.

References

Barajas-Olalde, C., *Davydycheva, S., Hanstein, T., Laudal, D., Martinez, Y., MacLennan, K., Mikula, S., Adams*, D.C., Klapperich, R.J., Peck, W.D., and Strack, K., 2021, Using controlled-source electromagnetics (CSEM) for CO2 storage monitoring in North Dakota CarbonSafe project, Soc. Exppl. Geophys., Expanded abstract Annual Meeeting, 503-506, doi: 10.1190/segam2021-3585379.1.

Keller, G.V. and Frischknecht, F.C. , 1966, *Electrical Methods in Geophysical Prospecting*, *Pergamon Press*.

Strack, K.-M., 1992, Exploration with Deep Transient Electromagnetics . *Elsevier Science Publishers B. V.,* Amsterdam. (copyright released version available at www.kmstechnologies.com/ Publications.html#1992)